

**WHY THE SOUND-ABSORBING PERFORMANCE OF HEARTWOOD
AND SAPWOOD DIFFERS IN YELLOW POPLAR (*LIRIODENDRON TULIPIFERA*)
CROSS-SECTIONS?**

EUN-SUK JANG, CHUN-WON KANG
JEONBUK NATIONAL UNIVERSITY
REPUBLIC OF KOREA

(RECEIVED AUGUST 2021)

ABSTRACT

In this study, we investigated why the sound-absorbing performance is different with between heartwood and sapwood of yellow poplar, which are known for their sound-absorbing properties. We performed image observation as well as gas permeability, pore size, and porosity analysis, and measured the sound absorption coefficient of all samples using an impedance tube. We determined that the pores were significantly larger, and the gas permeability and through-pore porosity much higher, in the sapwood than the heartwood. The average sound absorption coefficient of the sapwood at 2000-6400 Hz (0.61 ± 0.04) was 2.7x that of the heartwood (0.23 ± 0.03). The average NRC of the sapwood (0.23 ± 0.01) was 1.9x that of the heartwood (0.12 ± 0.01). This study ultimately determined that the sapwood, as a consequence of its larger pore size and superior through-pore porosity, which thereby improved its gas permeability, outperformed the heartwood in terms of sound-absorption. We also determined that pore size and through-pore porosity were the primary parameters that determined the sound-absorbing performance of yellow poplar cross-sections.

KEYWORDS: Through-pore porosity, pore size, sound absorption coefficient, yellow poplar.

INTRODUCTION

Noise pollution, like the problem of global warming, has attracted the attention of researchers worldwide (Anees et al. 2017). In Korea in particular, the number of civil complaints filed protesting indoor noise has steadily increased along with urbanization and population density (Kim 2015). As COVID-19 has required more Koreans to remain indoors for longer, the opportunity for disputes over noise between neighbors has increased (Yildirim and Arefi 2021).

To solve global warming and reduce noise pollution, a number of researchers have proposed the accelerated use of wood, known for its porosity, as an eco-friendly sound absorbing material (Chung et al. 2017, Jayamani et al. 2013, Kang et al. 2008, 2010, 2021a,b, Kolya and Kang 2020, 2021a,b, Wang et al. 2014, Wassilieff 1996). Researchers have also concentrated on maximizing wood's sound-absorbing performance through physicochemical treatments (Kang et al. 2019, 2021a, Kolya and Kang 2021a, Wang et al. 2014).

Kang et al. (2010) reported on the anatomical characteristics of wood with an excellent capacity for sound-absorption, suggesting that the presence of large vessels and diffuse-porous connections between these vessels via a simple perforated plate are most advantageous. In short, how well wood performs at sound-absorbing is related to its gas permeability. This makes sense, as a highly permeable sound absorbing material has a wide void volume that allows for maximum sound penetration (Kang et al. 2020, Taghiyari et al. 2014, Tang et al. 2018).

Kang et al. (2020) investigated the relationship between gas permeability and sound absorption coefficient in heartwood and sapwood from Japanese Sugi, Chanchin-modoki, and Yurinoki, reporting a higher gas permeability in sapwood than in heartwood, and corresponding improvements the sound absorption coefficient. Jang et al. (2019) classified the porosity of yellow poplar heartwood and sapwood, examining the percent of through pores, blind pores, and closed pores, finding that pore size, through-pore porosity, and gas permeability were higher sapwood than heartwood. Jang et al. (2020) subsequently investigated pore size and porosity of three species of softwood, finding that in softwood permeability in the fiber direction was affected by pore size and through-pore porosity.

Based on these previous studies, we predicted that larger pore size and higher through-pore porosity would enhance sound absorbing performance. Accordingly, the gas permeability, pore size, and porosity of heartwood and sapwood specimens from a yellow-poplar were analyzed. Using this data, we assessed the effect of pore structure on sound absorption performance.

MATERIALS AND METHODS

Specimen preparation

For this study, a natural dried state log of yellow poplar (*Liriodendron tulipifera*) approximately 20 years-old was supplied from Saehan Timber Co., Ltd (Korea). The cross-sectioned the log into samples were cut 1 cm thick. In order to sound absorption coefficient measurement consistent with ISO 10534-2, circular specimens of heartwood and sapwood with a diameter of 2.9 cm were taken. Ten samples (without cracks and knots) each of heartwood and sapwood were selected. Fig. 1 depicts the sample preparation process used in this study. The moisture content of the specimens was average 6.87% (heartwood) and 6.67% (sapwood).



Fig. 1: Sample preparation (top line: heartwood, bottom: sapwood).

Observation of vessels by scanning electron microscope (SEM)

The heartwood and softwood vessels were examined with a scanning electron microscope (SEM) (Genesis-1000, Emcrafts, Sungnam, Korea). After softening the specimens, the surface was shaved with a microtome and coated with gold. The cross-section and tangential section of each specimen was then observed at 500× magnification.

Permeability and porosity analysis

Gas permeability may be assessed using any of the various methods developed by Darcy, Frazier, or Gurley, or using air resistance (Kleinschmidt 1999, Landsberg and Winston 1947, Pacella et al. 2011). In this study, Darcy permeability was selected, as this is the most commonly used means of assessment (Kolya and Kang 2021a, Panigrahi et al. 2018). Eq. 1 yields the Darcy permeability constant:

$$C = 8FTV/\pi D^2(P^2 - 1) \quad (1)$$

where: C - Darcy permeability constant; F - flow; T - sample thickness; V - viscosity of air; D - sample diameter; and P - pressure.

Air pressure range for Darcy permeability was 0 to 1 bar in the longitudinal direction. The Darcy permeability of each specimen was measured by capillary flow porometer (model: CFP-1200AEL, Porous Material Inc., Ithaca, USA). Pore size can be assessed by imaging, mercury intrusion porosimetry, or capillary flow porometry (Guo et al. 2020, Jang and Kang 2020, Jang et al. 2018, Plötze and Niemz 2011). In this study, capillary flow porometry was selected, which is based on ASTM F-316 and measures only the constricted parts of the through pores. Maximum pore size and mean pore size were calculated by bubble point and the mean flow pore pressure, respectively. Eq. 2 provides pore size calculation by capillary flow porometer (model: CFP-1200AEL, Porous Material Inc., Ithaca, USA):

$$D = \frac{C\tau}{p} \quad (2)$$

where: D - limiting diameter, τ - surface tension, p - pressure, and C - constant of 2860 when p is measured in Pa, 2.15 when p is measured in cm Hg, and 0.415 when p is measured in psi units.

The proportion of pores that comprise the total volume of a sample is defined as porosity. Pores are classifiable into three types on the basis of shape: through pores with both ends open, blind pores with only one end open, and closed pores, which are surrounded and have no external interaction (Rouquerol et al. 1994). Wood substance density was estimated to be 1.5 g.cm^{-3} (Lindgren 1991), while total porosity (Φ_{total}) was calculated according to Eq. 3:

$$\phi_{\text{total}} (\%) = \left(1 - \frac{\rho_{\text{bulk}}}{1.5}\right) \times 100 \quad (3)$$

where: ρ_{bulk} - bulk density

Fig. 2 depicts pore classification. Porosity analysis in this study was performed consistent with a method of distinguishing between the three types of pores proposed by the authors in a prior study (Jang and Kang 2019, Jang et al. 2019, 2020). First, the open-pore porosity (Φ_{open}) of the cylindrical specimen was measured by gas pycnometer (Model: PYC-100A-1, Porous Materials Inc, USA) consistent with ISO 12154. The closed pore porosity (Φ_{closed}) was calculated as the difference between the total porosity and the open pore porosity (Eq. 4):

$$\phi_{\text{closed}} (\%) = \phi_{\text{total}} - \phi_{\text{open}} \quad (4)$$

The circular specimen was immersed in Galwick solution, which has a very low surface tension (0.159 N.m^{-1}) and easily penetrates open pores. The wetted circular specimen was placed into the sample chamber, and when air was applied in the fiber direction the Galwick solution in the through pores was extruded. In this manner, blind pore porosity (Φ_{blind}) was calculated as the difference between the weight of the dry circular specimen and the weight of the specimen after the Galwick solution was extruded. Through pore porosity (Φ_{through}) is the difference between open-pore porosity and blind-pore porosity (Eq. 5):

$$\phi_{\text{through}} (\%) = \phi_{\text{open}} - \phi_{\text{blind}} \quad (5)$$

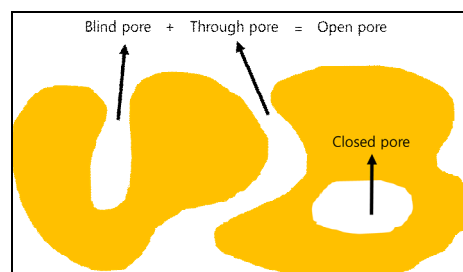


Fig. 2: Classification of pores on the basis of their physical shape.

Sound absorption coefficient measured by impedance tube

The sound absorption coefficient of the circular specimens was measured at 100-6400 Hz using a small impedance tube (model: type 4206, Brüel & Kjær, Denmark) consistent with

ISO 10534-2. An O-ring was inserted to close the fine gap between the circular specimen and the wall of the impedance tube (Kang et al. 2021b).

Using raw data concerning the sound absorption coefficient, the noise reduction coefficient (NRC), which is an average of the sound absorption coefficient at 250, 500, 1000, and 2 000 Hz, was calculated using raw data concerning the sound absorption coefficient, consistent with ISO 11654. The average of the sound absorption coefficient was calculated for the following frequency ranges: 250-500, 500-1000, 1000-2000, 2000-6400 Hz.

Statistical analysis

The effect of pore structure on the sound absorption coefficient of yellow poplar was analyzed statistically. Pearson's correlation coefficient was calculated to determine the degree and direction of the correlation between sound absorption, through pore porosity, blind pore porosity, closed pore porosity, and pore size.

RESULTS AND DISCUSSION

SEM images of heartwood and sapwood

Fig. 3 depicts the morphology of the cross-section and tangential-section of yellow poplar's heartwood and sapwood. The vessel arrangement observed is typical of diffuse-porous woods. Their perforation plate was scalariform, with a few tyloses observed in the heartwood. In the tangential section, tyloses were septa-like (De Micco et al. 2016), however the sapwood vessels were clean.

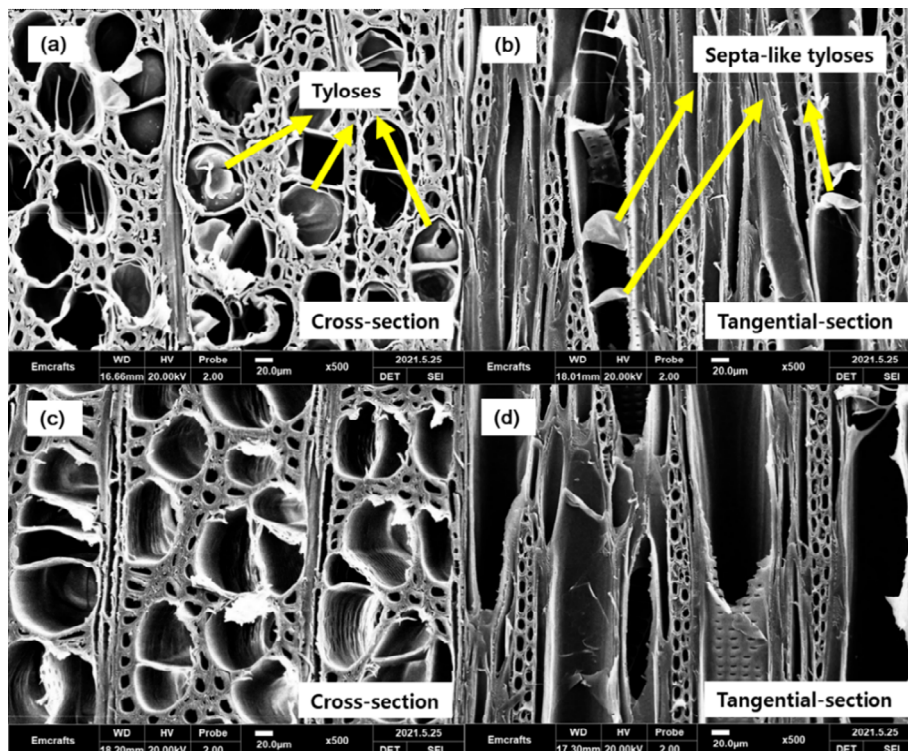


Fig. 3: SEM images of yellow poplar (top: heartwood, bottom: sapwood).

Gas permeability, pore size and porosity analysis

Fig. 4 presents the gas permeability, pore size, and porosity of the yellow poplar. Heartwood permeability was 0.42 ± 0.19 Darcy, while sapwood was 29.47 ± 4.33 Darcy. The gas permeability of sapwood, in other words, is 70x higher than that of sapwood. This is attributed to the development of tyloses in the heartwood (Bao et al. 1999, Jang et al. 2019, Jang et al. 2020, Kang et al. 2020).

The maximum pore size found in the heartwood was 11.42 ± 3.10 μm while the mean pore size was 1.32 ± 0.53 μm , while in the sapwood the maximum pore size was 28.65 ± 0.77 μm and the mean pore size was 10.74 ± 1.35 μm . The pore maximum pore size in the sapwood was 2.5x that of the pores in the heartwood, while the average pore size was 8.1x times more than that of the heartwood. Gas permeability is affected by the presence of through pores; as more tyloses develop, the through pores in the heartwood become more constricted, reducing permeability.

The difference in porosity between the heartwood and the sapwood was insignificant. Total porosity of the heartwood was 67.98 ± 1.97 μm , while that of the sapwood was 70.20 ± 1.09 μm . The through-pore porosity of the heartwood, however, was $19.33 \pm 3.16\%$, while that of the sapwood was $44.57 \pm 2.60\%$ (2.3x that of heartwood). In conclusion, both pore size and through-porosity of yellow poplar heartwood effected gas permeability (Jang and Kang 2019, Jang et al. 2019).

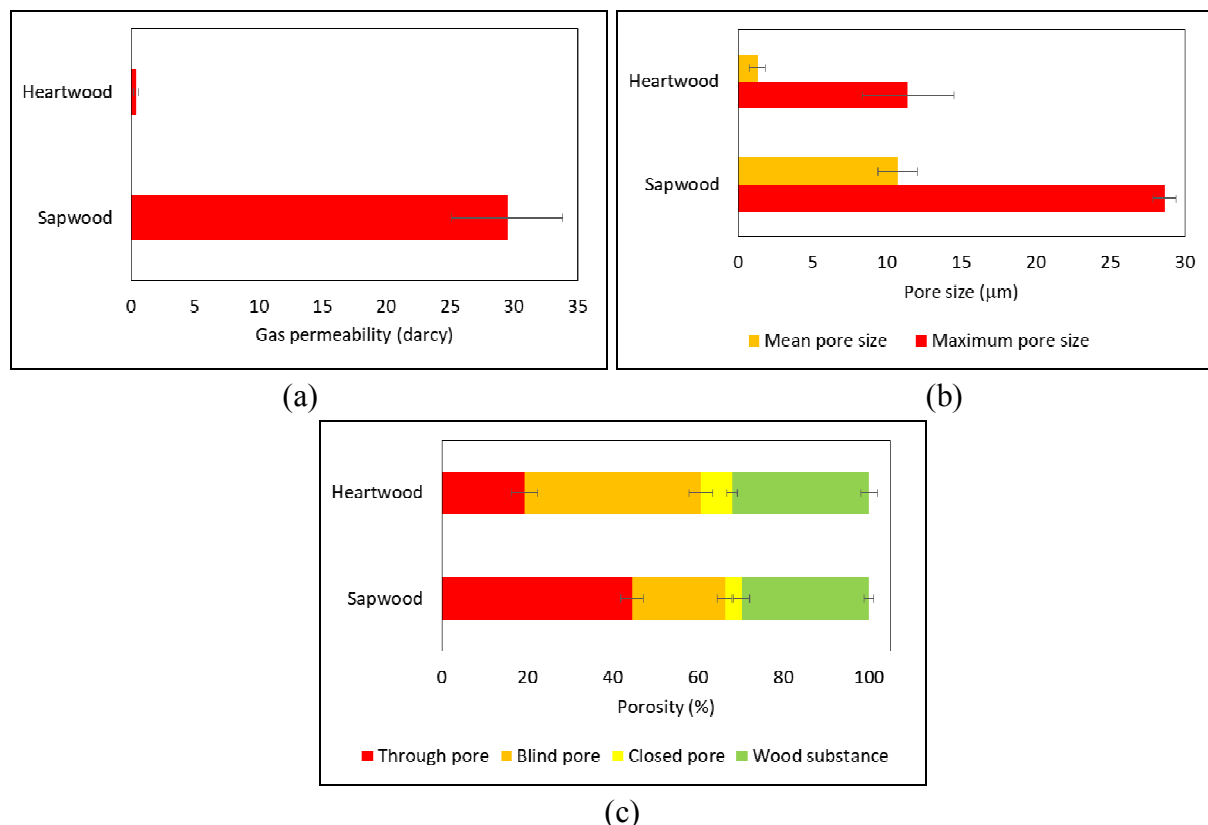


Fig. 4: Results of gas permeability tests: a) pore size, b) porosity, c) depending on heartwood and sapwood of yellow poplar. (Error bar is standard deviation).

Sound absorption coefficient

Fig. 5 shows the average sound absorption coefficient curve of heartwood and sapwood between 100 to 6400 Hz by small impedance tube. Tab. 1 provides the average NRC and sound absorption coefficient within each tested frequency range for the heartwood and sapwood.

At 250-500 Hz there was little difference in the sound absorption coefficient of the heartwood and sapwood. However, the average sound absorption coefficient at 2 000-6400 Hz of the sapwood (0.61 ± 0.04) was 2.7x that of the heartwood (0.23 ± 0.03). Ultimately, the average NRC of the sapwood (0.23 ± 0.01) was 1.9x that of the heartwood (0.12 ± 0.01).

Both heartwood and sapwood's sound absorption coefficient curves were consistent with that of a typical porous sound-absorbing material, in which the sound absorbing coefficient increases as frequency increases (Egab et al. 2014). Overall, the sound absorbing performance of the sapwood was better than that of the heartwood.

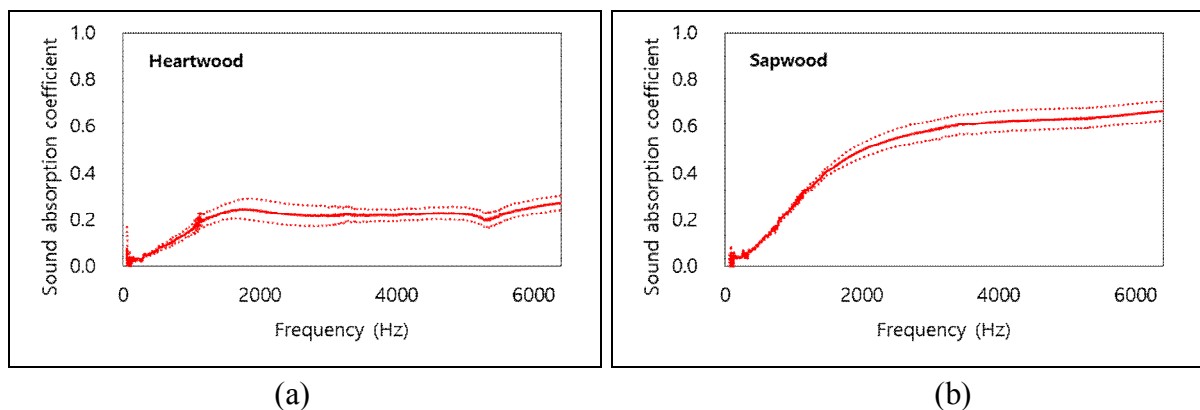


Fig. 5: Sound absorption coefficient curves of yellow poplar's heartwood (a) and sapwood (b). (Dotted line is standard deviation).

Tab. 1: Average NRC and sound absorption coefficient of yellow poplar's heartwood and sapwood.

Yellow poplar	NRC (-)	Average sound absorption coefficient (-)			
		250-500 Hz	500-1000 Hz	1 000-2 000 Hz	2 000-6 400 Hz
Heartwood	0.12	0.05	0.11	0.22	0.23
SD	0.01	0.01	0.02	0.03	0.03
Sapwood	0.23	0.07	0.18	0.40	0.61
SD	0.01	0.00	0.01	0.02	0.04

Statistical analysis

Tab. 2 presents the results of our Pearson's coefficient correlation analysis examining the relationship between the sound absorption coefficient within each frequency range and through-pore porosity, blind-pore porosity, closed-pore porosity, maximum pore size, and mean pore size. The correlation coefficients between maximum pore size, mean pore size, through-pore porosity, and average sound absorption coefficient within each frequency range showed a significant positive correlation at the 1% level, with the correlation coefficients moving higher at higher frequencies. In contrast, blind-pore porosity, closed-pore porosity and sound

absorption coefficient across each frequency range manifested a statistically significant negative correlation at the 1% significance level, with the negative correlation coefficient growing at higher frequencies.

Tab. 2: Pearson's coefficient correlation analysis.

Pore size and porosity	Average sound absorption coefficient (-)			
	250-500 Hz	500-1000 Hz	1000-2000 Hz	2000-6400 Hz
Maximum pore size	.830**	.931**	.959**	.962**
Mean pore size	.856**	.918**	.932**	.952**
Through pore porosity	.832**	.929**	.973**	.977**
Blind pore porosity	-.810**	-.911**	-.970**	-.973**
Closed pore porosity	-.636**	-.710**	-.733**	-.723**

Note: ** represents a significance at 1% levels.

In sum, the yellow poplar's porosity and pore size differ in their effects on the sound absorption coefficient; pore size and through pore porosity increase sound absorbing performance, while blind pore porosity and closed pore porosity inhibit sound absorbing performance in yellow poplar cross sections.

Pore size and through pore porosity are determined by gas permeability. Sound absorbing performance is closely related to gas permeability. Logically, therefore, as pore size grows and through pore porosity increases, sound absorbing performance improves.

One limitation of this study is that only samples of yellow poplar were measured. We leave it for other researchers to determine the pore structure of other wood species and their relationship with the sound-absorbing performance of those species.

CONCLUSIONS

The pore structure and sound-absorbing performance of yellow poplar heartwood and sapwood cross sections were examined. Pore sizes were larger and through pore porosity was higher in sapwood than in heartwood, a difference which we attribute to the physical pore structure (allowing for more gas permeability) in the former. Yellow poplar exhibited improved sound absorbing properties at higher frequencies, with the sapwood manifesting greater capacity for sound absorption than heartwood. Improvements to pore size and through-pore porosity enhance sound-absorbing performance, while blind pore porosity and closed pore porosity inhibit sound-absorbing performance.

ACKNOWLEDGMENTS

This research was supported by a grant from the Basic Science Research Program of the National Research Foundation of Korea (NRF), funded by the Ministry of Education (NRF-2019R1I1A3A02059471). It was also supported a grant from the international cooperation program framework managed by the NRF (NRF-2020K2A9A2A08000181). The authors are also thankful to 'The Business Startup Incubator Support Program' supported by the Ministry of Education and National Research Foundation of Korea.

The data used in this article are part of the first author (EUN-SUK JANG)'s Jeonbuk National University doctoral dissertation.

REFERENCES

1. Anees, M.M., Qasim, M., Bashir, A., 2017: Physiological and physical impact of noise pollution on environment. *Earth Science Pakistan* 1(1): 08-11.
2. ASTM F316-03, 2019: Standard test methods for pore size characteristics of membrane filters by bubble point and mean flow pore test.
3. Bao, F., Lu, J., Avramidis, S., 1999: On the permeability of main wood species in China. *Holzforschung* 53(4): 350-354.
4. Chung, H., Park, Y., Yang, S.Y., Kim, H., Han, Y., Chang, Y.S., Yeo, H., 2017: Effect of heat treatment temperature and time on sound absorption coefficient of *Larix kaempferi* wood. *Journal of Wood Science* 63(6): 575-579.
5. De Micco, V., Balzano, A., Wheeler, E.A., Baas, P., 2016: Tyloses and gums: a review of structure, function and occurrence of vessel occlusions. *IAWA journal* 37(2): 186-205.
6. Egab, L., Wang, X., Fard, M., 2014: Acoustical characterisation of porous sound absorbing materials: a review. *International Journal of Vehicle Noise and Vibration* 10(1-2): 129-149.
7. Guo, L., Cheng, H., Chen, J., Chen, W., Zhao, J., 2020: Pore structure characterization of oak via X-ray computed tomography. *BioResources* 15(2): 3053-3063.
8. ISO 10534-2, 2001: Acoustics. Determination of sound absorption coefficient and impedance in impedance tubes. Part 2 transfer-function method.
9. ISO 11654, 1997: Acoustics. Sound absorbers for use in buildings. Rating of sound absorption.
10. ISO 12154, 2014: Determination of density by volumetric displacement. Skeleton density by gas pycnometry.
11. Jang, E.S., Kang, C.W., 2019: Changes in gas permeability and pore structure of wood under heat treating temperature conditions. *Journal of Wood Science* 65(1): 1-9.
12. Jang, E.S., Kang, C.W., 2020: Do face masks become worthless after only one use in the covid-19 pandemic? *Infection & Chemotherapy* 52(4): 583-591.
13. Jang, E.S., Kang, C.W., Jang, S.S., 2018: Comparison of the mercury intrusion porosimetry, capillary flow porometry and gas permeability of eleven species of Korean wood. *Journal of the Korean Wood Science and Technology* 46(6): 681-691.
14. Jang, E.S., Kang, C.W., Jang, S.S., 2019: Pore characterization in cross section of yellow poplar (*Liriodendron tulipifera*) wood. *Journal of Korean Wood Science and Technology* 47(1): 8-20.
15. Jang, E.S., Yuk, J.H., Kang, C.W., 2020: An experimental study on change of gas permeability depending on pore structures in three species (hinoki, Douglas fir, and hemlock) of softwood. *Journal of Wood Science* 66(1): 1-12.

16. Jayamani, E., Hamdan, S., Suid, N.B., 2013: Experimental determination of sound absorption coefficients of four types of Malaysian wood. In: Applied Mechanics and Materials. Trans Tech Publications. Pp 577-581.
17. Kang, C.W., Jang, E.S., Hasegawa, M., Matsumura, J., 2020: Studies of the relationship between sound absorption coefficient and air permeability of wood. Journal of the Faculty of Agriculture Kyushu University 65(2): 351-355.
18. Kang, C.W., Jang, E.S., Jang, S.S., Cho, J.I., Kim, N.H., 2019: Effect of heat treatment on the gas permeability, sound absorption coefficient, and sound transmission loss of *Paulownia tomentosa* wood. Journal of the Korean Wood Science and Technology 47(5): 644-654.
19. Kang, C.W., Jang, E.S., Lee, N.H., Jang, S.S., Lee, M., 2021a: Air permeability and sound absorption coefficient changes from ultrasonic treatment in a cross section of Malas (*Homalium foetidum*). Journal of Wood Science 67(1): 1-5.
20. Kang, C.W., Kang, W., Chung, W.Y., Matsumura, J., Oda, K., 2008: Changes in anatomical features, air permeability and sound absorption capability of wood induced by delignification treatment. Journal of the Faculty of Agriculture Kyushu University 53(2): 479-483.
21. Kang, C.W., Kang, W., Kim, G.C., 2010: Sound absorption capability and anatomical features of highly sound absorptive wood. Journal of the Korean Wood Science and Technology 38(4): 292-297.
22. Kang, C.W., Kolya, H., Jang, E.S., Zhu, S., Choi, B.S., 2021b: Steam exploded wood cell walls reveals improved gas permeability and sound absorption capability. Applied Acoustics 179(108049).
23. Kim, K., 2015: Sources, effects, and control of noise in indoor/outdoor living environments. Journal of the Ergonomics Society of Korea 34(3): 265-278.
24. Kleinschmidt, K., 1999: A simple tool for classifying the acoustical performance of permeable materials. Building Acoustics 6(1): 63-70.
25. Kolya, H., Kang, C.W., 2020: High acoustic absorption properties of hackberry compared to nine different hardwood species: A novel finding for acoustical engineers. Applied Acoustics 169(107475).
26. Kolya, H., Kang, C.W., 2021a: Effective changes in softwood cell walls, gas permeability and sound absorption capability of *Larix kaempferi* (larch) by steam explosion. Wood Material Science & Engineering 1-9.
27. Kolya, H., Kang, C.W., 2021b: Hygrothermal treated paulownia hardwood reveals enhanced sound absorption coefficient: An effective and facile approach. Applied Acoustics 174(107758).
28. Landsberg, M., Winston, G., 1947: Relationship between measurements of air Permeability by two machines. Textile Research Journal 17(4): 214-221.
29. Lindgren, L., 1991: Medical CAT-scanning: X-ray absorption coefficients, CT-numbers and their relation to wood density. Wood Science and Technology 25(5): 341-349.

30. Pacella, H.E., Eash, H.J., Frankowski, B.J., Federspiel, W.J., 2011: Darcy permeability of hollow fiber bundles used in blood oxygenation devices. *Journal of Membrane Science* 382(1-2): 238-242.
31. Panigrahi, S., Kumar, S., Panda, S., Borkataki, S., 2018: Effect of permeability on primary processing of wood. *Journal of Pharmacognosy and Phytochemistry* 7(4): 2593-2598.
32. Plötze, M., Niemz, P., 2011: Porosity and pore size distribution of different wood types as determined by mercury intrusion porosimetry. *European Journal of Wood and Wood Products* 69(4): 649-657.
33. Rouquerol, J., Avnir, D., Fairbridge, C., Everett, D., Haynes, J., Pernicone, N., Ramsay, J., Sing, K., Unger, K., 1994: Recommendations for the characterization of porous solids (Technical Report). *Pure and Applied Chemistry* 66(8): 1739-1758.
34. Taghiyari, H., Zolfaghari, H., Sadeghi, M., Esmailpour, A., Jaffari, A., 2014: Correlation between specific gas permeability and sound absorption coefficient in solid wood. *Journal of Tropical Forest Science* 26(1): 92-100.
35. Tang, X., Jeong, C.H., Yan, X., 2018: Prediction of sound absorption based on specific airflow resistance and air permeability of textiles. *The Journal of the Acoustical Society of America* 144(2): EL100-EL104.
36. Wang, D., Peng, L., Zhu, G., Fu, F., Zhou, Y., Song, B., 2014: Improving the sound absorption capacity of wood by microwave treatment. *BioResources* 9(4): 7504-7518.
37. Wassilieff, C., 1996: Sound absorption of wood-based materials. *Applied Acoustics* 48(4): 339-356.
38. Yildirim, Y., Arefi, M., 2021: Noise complaints during a pandemic: A longitudinal analysis. *Noise Mapping* 8(1): 108-115.

EUN-SUK JANG, CHUN-WON KANG*
JEONBUK NATIONAL UNIVERSITY
INSTITUTE OF HUMAN ECOLOGY, COLLEGE OF HUMAN ECOLOGY
DEPARTMENT OF HOUSING ENVIRONMENTAL DESIGN AND RESEARCH
567, BAEKJE-DAERO, DEOKJIN-GU 54896
JEONJU-SI, JEOLLABUK-DO.
REPUBLIC OF KOREA

*Corresponding author: kewon@jbnu.ac.kr